

Enhanced Conductivity and Fluorescence of Polyaniline Doped with Eu^{3+} , Tb^{3+} , and Y^{3+} Ions

Jiali Zhang, Hao Wang, Shimei Yang, Shaohui Wang, Shaoming Yang

Department of Chemistry and Chemical Engineering, East China Jiaotong University, Nanchang 330013, P.R. China

Received 2 June 2011; accepted 19 November 2011

DOI 10.1002/app.36516

Published online 22 January 2012 in Wiley Online Library (wileyonlinelibrary.com).

ABSTRACT: The doped polyaniline (PANI) with rare earth ions, which exhibits an increasing conductivity and strongly enhanced fluorescence emission, was prepared by dispersing PANI powder suspension in acetonitrile solution containing rare earth ions according to different mass ratios of rare earth ions to PANI at room temperature. The structure of the doped PANI was characterized by the spectra of FTIR, Raman, UV-vis, and XRD. Red-shifted change for the quinoid and benzenoid stretching vibration is observed in IR and Raman spectra after doping rare earth cations, and UV-vis absorption peak also presents a red-shift, indicating that the doped PANI possesses a better delocalization of electrons along the mainchain

backbone. The experimental data show that the electrical and optical behaviors of PANI strongly depend on the species of rare earth cations and their concentration. It is found that enhancing fluorescence for the doped PANI is observed by comparing with emeraldine base (EB). Moreover, the conductivity of the protonated PANI samples doped with Eu^{3+} , Tb^{3+} , and Y^{3+} ions, increases from 2.1×10^{-4} to 3.33 S cm^{-1} , $1.50 \times 10^{-1} \text{ S cm}^{-1}$ and $2.26 \times 10^{-1} \text{ S cm}^{-1}$. © 2012 Wiley Periodicals, Inc. *J Appl Polym Sci* 125: 2494–2501, 2012

Key words: polyaniline; rare earth ions; conductivity; fluorescence

INTRODUCTION

Polyaniline (PANI) has been most extensively studied since it exhibits good environmental stability, facile synthesis, electrical and optical properties, and unique doping/de-doping behavior.^{1,2} Its electrical properties can be reversibly modulated by both the oxidation state of the polymeric chains and protonation. The conducting form of PANI is considered as emeraldine salt (ES) through doping emeraldine base (EB) with protonic acids. The doping process occurs at imine nitrogen atoms accompanied with an internal redox reaction that results in the formation of semiquinone segments. Additionally, another dopant, such as transition metal,^{3–6} and alkali metal,^{7,8} can also be employed to achieve high conductivity through interaction with nitrogen atoms of polyaniline backbone. The doping mechanisms of EB with metal ions present two interaction formulas on the polymer backbone. One of mechanisms is similar to EB doped by mineral acid, such as alkali metal ions, and nonactive redox ions, but the process is not redox or direct electron transfer between the metal ion and EB, which is called pseudo-protonation.^{8–10} However, in the case of transi-

tion metal ions, the interaction with amine nitrogen atoms on the chain backbone is considered two-step redox process,^{11,12} as well as the mechanism of pseudo-protonation. The doping process occurs through the oxidation of amine nitrogen atom by metal cation, and radical cation segments on the chain backbone is obtained by transition metal ions oxidizing amine nitrogen atoms. Although the f-f electronic transitions of rare earth element are relatively insensitive to perturbation in their chemical environment, the interactions of organic polymer with rare earth ions can result in the change of electrical and optical properties. Therefore, the complex formation of rare earth ions with organic polymer is particularly interesting. For example, Chen¹³ had investigated the conductivity of polyacetylene film doped by anhydrous rare earth chloride, showing 1–3 orders of magnitude higher conductivity after doping rare earth ions than original polyacetylene film. This complex of conjugated organic polymers with divalent europium exhibits a high quantum efficiency in the solid state.¹⁴ In the work, we report the synthesis, formation and some electrical and optical properties of PANI-rare earth ions through studying the mass ratio of PANI to rare earth ions and the interaction between PANI and rare earth ions.

Correspondence to: J. Zhang (zhangjiajiali@163.com).

Contract grant sponsor: National Natural Science Foundation of China; contract grant number: 21164001.

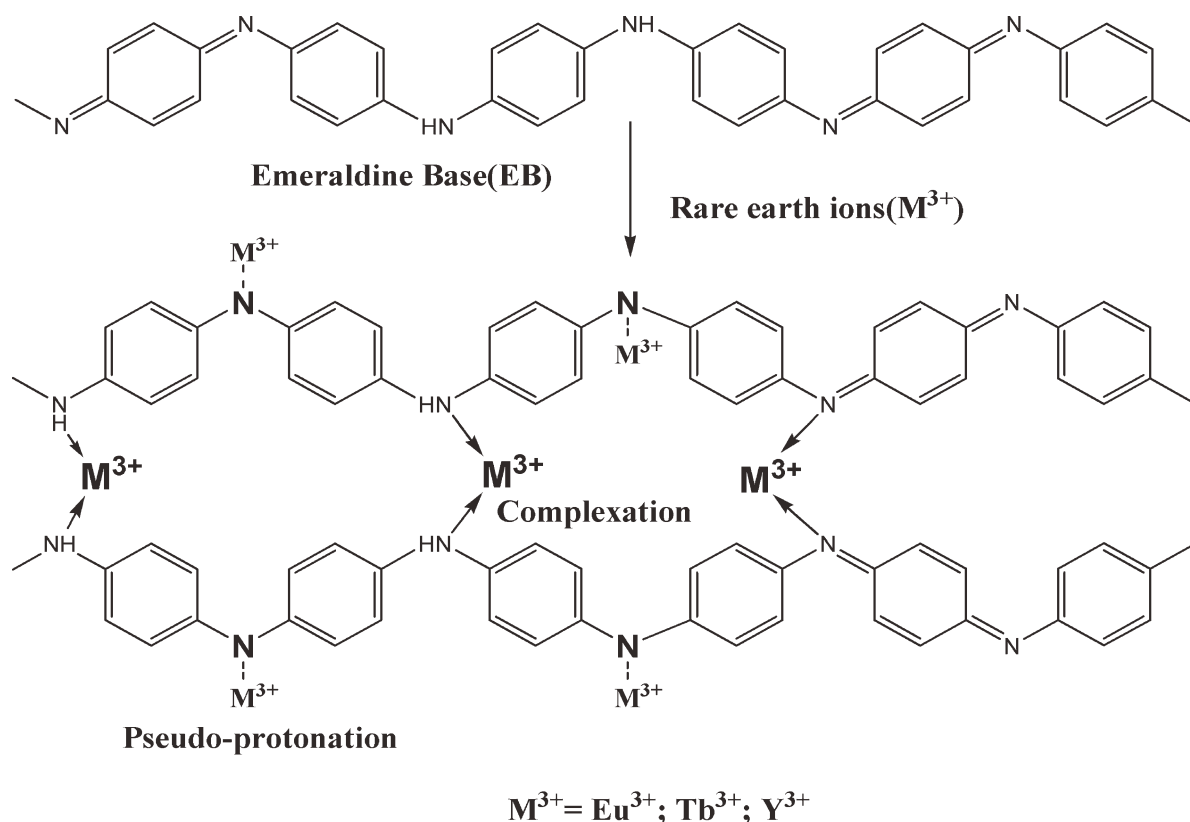
Contract grant sponsor: Natural Science Foundation of Jiangxi Province, China; contract grant number: 2010GZH0029.

Journal of Applied Polymer Science, Vol. 125, 2494–2501 (2012)
© 2012 Wiley Periodicals, Inc.

EXPERIMENT

Materials

Aniline was purified by repeated distillation and stored under nitrogen in the dark. All other reagents



Scheme 1 The structure of Polyaniline prepared by a chemically oxidative polymerization and the redox, complexation and *pseudo*-protonation process after doping with rare earth ions.¹¹

(Eu_2O_3 , Tb_4O_7 , Y_2O_3 , etc.) were of analytical reagent grade and used as received. All solutions were prepared with deionized water.

Synthesis of the doped PANI

EB and its ES (PANI-HCl) forms were prepared by the oxidative polymerization of aniline using ammonium peroxydisulfate in 1M HCl solution. A typical preparation procedure is as follows: 3.723 mL (0.04 mol) of aniline and 20 mL of 1M HCl were mixed in a 100 mL glass beaker. Ammonium persulfate (9.128 g, 0.04 mol) was dissolved in 30 mL of 1M HCl as oxidant solution. The oxidant solution was slowly dropped into the monomer solution with magnetic stirring. The resulting product presents a dark blue powder, which is called emeraldine salt (ES). The synthesis of emeraldine base (EB) adopts a conventional method by deprotonated with excess 0.1M NH_4OH solution.

To exclude the influence of different counter-ions, the rare-earth oxide was first dissolved in the hot concentrated HCl. An anhydrous rare earth chloride salt was obtained by using vacuum dry to remove water from solution. The PANI doped with rare earth ions has been carried out in acetonitrile solution containing different amount of rare earth ions according to the certain mass ratio (0.5, 1, 1.5, 2, 2.5)

of rare earth ions to PANI at room temperature. The suspension of PANI powder is maintained for 12 h under constant stirring, and then the precipitate is filtered and washed with 95% ethanol several times, finally the obtained product was dried at 60°C for 24 h. The resulting powder samples were labeled as Eu-PANI, Tb-PANI, and Y-PANI, respectively.

Measurements

The doping contents of Eu^{3+} , Tb^{3+} , and Y^{3+} ions in the sample were determined by conductively coupled plasma atomic emission spectrometer (ICP, Model 720-ES, VARIAN, USA). Fourier transform infrared (FTIR) spectra of all samples were recorded on a PerkinElmer FTIR spectrometer in KBr pellets. The UV/vis absorption spectrum of all samples dissolved in *N*-methylpyrrolidone was recorded on a PerkinElmer Lambda 35 spectrophotometer. Raman spectra were measured in a FT-Raman Bruker SENTERRA Spectrometer with 1064 nm excitation radiation. In this case, laser power was always kept below 20 mW to avoid sample degradation. The resolutions of the IR spectrometer and the Raman spectrophotometer were 2.0 and 0.2 cm^{-1} , respectively. Emission and excitation spectra of all samples dissolved in NMP at room temperature were collected by means of a Cary Eclipse spectrophotofluorometer

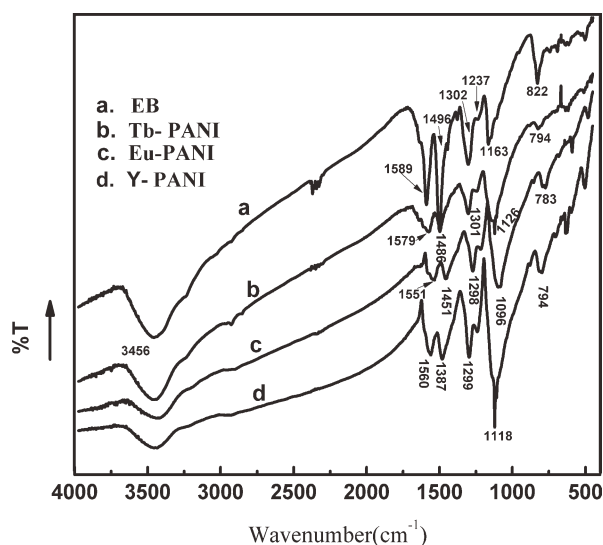


Figure 1 FTIR spectra of EB(a) and the doped PANI powder with (b) terbium ion; (c) europium ion; (d) yttrium ion, respectively, at the mass ratio of rare earth ion to PANI for 2.5.

using the corresponding excitation wavelength with 2.5 nm slits. X-ray diffraction (XRD) was carried out using a D/max 2550 model X-ray diffractometer (Bruker) with CuK α radiation at a scanning rate of 10°min⁻¹ in the reflection mode over a 2 θ range from 5 to 70°. PANI doped by rare earth ions was pressed into a pellet of 10 mm diameter and ca. 2 mm thickness under pressure. The conductivity of PANI pellets was measured using RTS-8 four probe conductivity meter at room temperature.

RESULTS AND DISCUSSION

Characterization of the doping PANI

The different IR vibration characteristics spectra of the doped PANI that was prepared by the mass ratio of the rare earth ions to PANI for 2.5 in acetonitrile solution, are showed in Figure 1. Five essential absorption bands centered around 1589, 1496, 1302, 1163, 822 cm⁻¹ are observed. It is indicated that protonated reaction is main in polymeric chains.¹⁵ Com-

paring to EB, some shifted-bands in the spectra of PANI doped with the rare earth ions are able to be observed, as shown in Table I. In all doping experiments, the typical absorption bands assigned to N=Q=N stretching vibration at 1589 cm⁻¹ and N-B-N stretching vibration at 1496 cm⁻¹ shifted to lower frequency after the PANI was doped with Eu³⁺, Tb³⁺, and Y³⁺ ions, respectively, while the absorption peaks for Eu-PANI and Tb-PANI present at higher vibration frequency. The results suggest that the red shift of the IR absorption peaks is referred to be a signature of the conversion of the quinoid rings to the benzenoid rings due to proton-induced spin-unpairing mechanism,¹⁶ which was considered to be an indication of increasing degree of charge delocalization on the polyaniline backbone due to protonation.¹⁷ Also, the IR shift indicates that the degree of charge delocalization of polymerization increases with the doping of the rare earth ions, and the rare earth ions were introduced into polyaniline backbone by complexation or pseudo-protonation process of the imine nitrogen.¹⁸ The fact was also validated by the experiment of inductively coupled plasma emission spectrometer (ICP), as shown in Table II. Compared to HCl-PANI in previously investigations,¹⁵ the band keeps unchanged in Eu-PANI, Y-PANI, and Tb-PANI. It implies that the imine sites are protonated preferentially in the case of protonation with simple inorganic acids. On the contrary, an obvious change, the band at 1163 cm⁻¹ assigned to Q=NH⁺-B bending mode shift to 1126, 1098, and 1118 cm⁻¹ after doping Tb³⁺, Eu³⁺, and Y³⁺, respectively, was observed in Figure 1. One possible reason for this red-shifted change may be ascribed to a decreasing amount of quinoid units in the polymer chains with the doping on polyaniline backbone. The red-shifted change seems to have no concern with the doping content for rare earth ions owing to the same bands being obtained for different doping contents in the IR spectra.

The Raman spectra of EB, Eu-PANI, Tb-PANI, and Y-PANI samples were also measured using 1064 nm excitation radiation, as shown in Figure 2. All samples (including EB, Eu-PANI, Tb-PANI, and

TABLE I
Main IR Vibrational Frequencies (cm⁻¹) and the Corresponding Assigned Modes of Samples EB-PANI, Tb-PANI, Eu-PANI, Y-PANI

EB	Tb-PANI	Eu-PANI	Y-PANI	Stretching mode
1589	1579	1551	1560	N=Q=N stretching
1496	1486	1451	1387	N-B-N stretching
1302	1301	1298	1299	N-H bending
1237	1247	1218	1236	C-N stretching
1163	1126	1098	1118	B-NH ⁺ -B or ^a Q=NH ⁺ -B
822	794	783	794	Out -of-plane C-H bending

^a Q denotes quinoid units of PANI; B denotes benzenoid units of PANI.

TABLE II
The Doping Content and Conductivity of PANI Doped with Eu^{2+} , Tb^{3+} , and Y^{3+} Ions

Rare earth ion/PANI mass feed ratio	Eu-PANI		Tb-PANI		Y-PANI	
	Eu^{3+} doping content (wt %)	Conductivity (S cm^{-1})	Tb^{3+} doping content (wt %)	Conductivity (S cm^{-1})	Y^{3+} doping content (wt %)	Conductivity (S cm^{-1})
0.0	0.00	2.10×10^{-4}	0.00	2.18×10^{-4}	0.00	2.18×10^{-4}
0.5	2.29	1.48×10^{-1}	2.80	5.54×10^{-3}	2.14	3.46×10^{-2}
1.0	6.18	1.89×10^{-1}	4.05	3.95×10^{-2}	3.84	8.49×10^{-2}
1.5	9.23	2.27×10^{-1}	4.48	6.72×10^{-2}	4.06	9.45×10^{-2}
2.0	10.12	2.53×10^{-1}	4.78	1.00×10^{-1}	6.01	1.39×10^{-1}
2.5	13.21	3.33×10^0	8.81	1.50×10^{-1}	9.88	2.26×10^{-1}

Y-PANI) dissolved in *N*-methylpyrrolidone (NMP) exhibited two absorption peaks locating at 331 and 628 nm in UV-vis spectrum in Figure 3. It implies that no resonance Raman spectra were observed using 1064 nm excitation radiation for the as-synthesized EB and the doping samples, which can effectively eliminate the fluorescent effect. The bands at 1612 cm^{-1} and 1576 cm^{-1} for EB assigned to C–C stretching of benzenoid units and C=C stretching of quinoid units, respectively, are observed in Figure 2(a). However, the former band appeared at 1619, 1624, and 1629 cm^{-1} in Figure 2(b–d), after treatment with Y^{3+} , Tb^{3+} , and Eu^{3+} ions, respectively, while the latter band disappeared, and the same behavior was observed for the band at 1486 cm^{-1} attributed to C=N stretching. In the case of the doped PANI, it can be seen that the high frequency of 1612 cm^{-1} band presents a blue shift phenomenon. Additionally, the band at 1225 cm^{-1} ($\nu\text{C-N}$ benzene diamine units) only appears in the Raman spectra of Figure 2(b–d), indicating a decrease in the amount of quinoid units due to the rare earth ion doping. One

possible reason of these changes with different degree for all doping samples may be because the degree of charge delocalization of PANI increase with the doping of the rare earth ions. Another fact that quinoid rings convert to benzenoid rings is the most characteristic Raman band of the radical cation (C–N+• stretching) observed at 1336 cm^{-1} . Comparing the Raman spectra in Figure 2(a) with those of in Figure 2(b–d), corresponding respectively to the C–H bending in the quinoid and the benzenoid segments,^{19–24} a small shift of the 1143 cm^{-1} band to 1151, 1148, and 1146 cm^{-1} was found. The bands between 800 and 900 cm^{-1} include much information about deformation of benzenoid rings, which also becomes more salient in all of the doping samples. The Raman results lead to the conclusion that the doping process with Y^{3+} , Tb^{3+} , and Eu^{3+} ions, respectively, in polyaniline induces not only conformational and structural changes of polymeric chains but also a transformation of quinoid units into semi-quinone ones.

Figure 3 compares UV-vis spectra of the EB and the doped PANI solution in NMP. The absorption spectra of EB solution show two distinct absorption

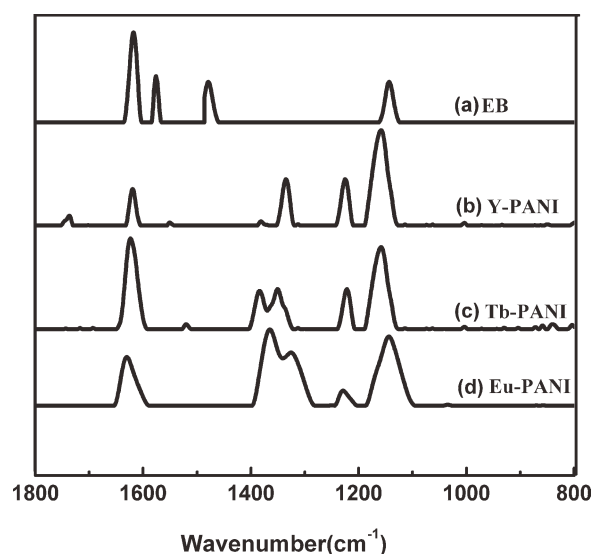


Figure 2 Raman spectra of EB(a) and the doped PANI powder prepared with (b) yttrium ion; (c) terbium ion; (d) europium ion, respectively, at the mass ratio of rare earth ion to PANI for 2.5.

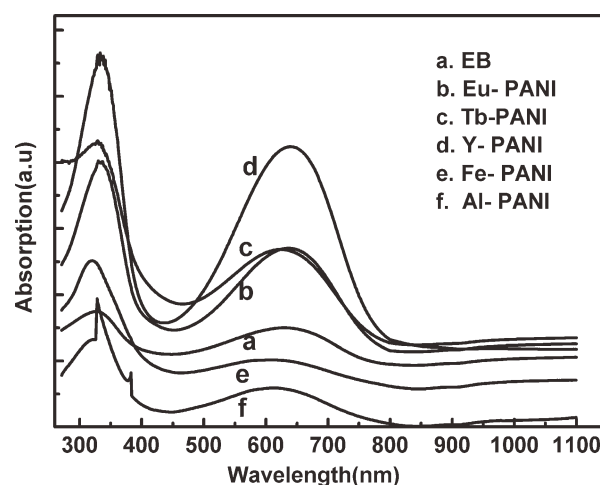


Figure 3 UV-visible absorption spectra of PANI doped with different rare earth ions in NMP. (a) emeraldine base; (b) europium ion; (c) terbium ion; (d) yttrium ion; (e) aluminum ion; (f) iron ion.

bands located at 328 and 620 nm. The former corresponds to the $\pi \sim \pi^*$ transition,^{21–24} whereas the absorption at 620 nm is associated with the presence of quinoid segments.²⁵ The peak assigned to the $\pi \sim \pi^*$ transition is shifted to 328–334 nm, and the other absorption peak relating to quinoid units will shift to 628–645 nm. The red-shifted wavelength mainly depends on the kind of the rare earth ions. This result may be attributed to the combination of the rare earth ions with polyaniline backbone. The red-shifts of these absorption bands indicate the better delocalization of electrons in the matrix of the doped polyaniline with Eu^{3+} , Tb^{3+} , and Y^{3+} ions. Some reasons for the better delocalization of electrons are as follows: (i) the trivalent rare earth ions have a very strong electronic inductive effect, and they can induce the π electrons to delocalize; (ii) the rare earth ions can complex with the amino and imine in the polymeric chains, and these interactions tend to form a bigger conjugate plane, thereby the better delocalization of electrons in the matrix of polyaniline after doping with the rare earth ions can be obtained. It can also be demonstrated by the changes of fluorescence spectra, due to the better delocalization of electrons, the intensity of polymeric fluorescence can get an enhancement after doping with the rare earth ions. However, the most shifted wavelength of PANI doped with Y^{3+} ions was observed, and this can be explained by the fact that Y^{3+} cations with close shell f-orbitals do not introduce low-energy metal-centered or charge-separated excited states comparing with Eu^{3+} and Tb^{3+} ions, so energy and electron-transfer processes cannot take place.²⁶ Comparing the UV-vis spectra of polyaniline doped with rare earth ions, their absorptions located at 620 nm shifted to lower wavelength for the Fe-PANI and Al-PANI. This blue-shifted peak can be ascribed to the Fe-PANI and Al-PANI have more quinone segments in their polymeric chains,²⁷ and their polymeric chains have a higher oxidation degree. It is also demonstrated that the conductivity of Fe-PANI with the higher oxidation degree is lower than that of the Al-PANI.

Figure 4 shows the X-ray diffraction patterns of EB, Y-PANI, Tb-PANI, and Eu-PANI powder. The polymer chains in a matrix generally include both amorphous and crystalline domains,^{21–24} and more highly ordered systems can exhibit a metallic-like conductivity state. As shown in Figure 4, in the case of the doped polyaniline two broad peaks centered at $2\theta = 20.8^\circ$ and 25.0° are observed, which are ascribed to the periodicity parallel and perpendicular to the polyaniline chains, respectively,^{21–24,28–31} whereas a more sharp diffractive peak is exhibited at $2\theta = 20.8^\circ$ in EB, the peak at 25.0° disappears. Additionally, a less sharp diffractive peak for the polymer doped with the rare earth ion is located at $2\theta = 5.8^\circ$, which

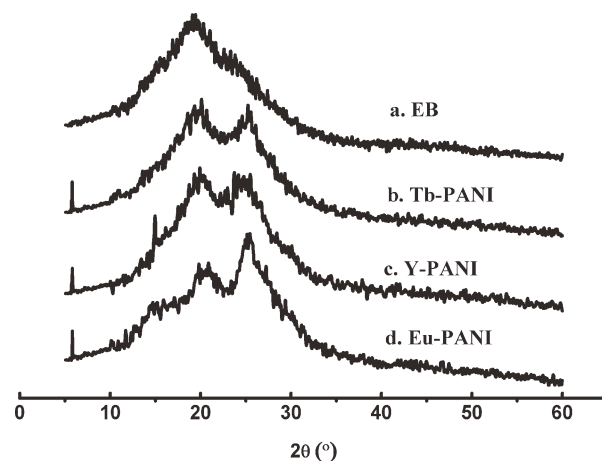


Figure 4 Wide-angle X-ray diffraction patterns of PANI powder doped with different rare earth ions. (a) emeraldine base; (b) terbium ion; (c) yttrium ion; (d) europium ion.

was assigned to the periodicity distance between the rare earth ion and nitrogen atom on adjacent polymer chains.²⁹ These results show that the ordering is higher for Y-PANI, Tb-PANI, and Eu-PANI powders than that of EB powders. The fact indicates that the structure of PANI chains will tend to organize the polymer chains in highly ordered arrays when the rare earth ions interaction with polymer, and a better periodicity perpendicular to the polymer chains is observed in the doped PANI possibly because of the rare earth ions cross-linking with adjacent polyaniline chains, indicating a larger periodicity distance in the doped PANI due to the interchain coordinating of the rare earth ions with adjacent polyaniline chains. It is the cooperative effect that results in more regularly and rigid PANI chains as doping Y^{3+} , Tb^{3+} , and Eu^{3+} ions, while the EB powder exhibits normally highly amorphous polymer.^{21–24,30,31} The WXRd result demonstrates that the doped polymer chains should be segregated, which leads to a more expanded and ordered matrix.

Electrical and optical properties of the doping PANI

To detect the change of conductivity of the doped polyaniline as the doping content, all samples are investigated by changing the metal cations concentration at a constant mass of polyaniline. The doping content of the cations in the sample is determined by conductively coupled plasma atomic emission spectrometer. The doping content and relating conductivity are listed in Table II. It shows that the doping contents of polyaniline depend on the kinds of cations and their concentration. The tendency of the doping content for various cations is almost the same, and the doping content increases as cations

concentration increases. A little change of the doping content occurs after the mass ratio of cations to PANI for 2.5, indicating that the contents of cations induced into polyaniline backbone are limited. Although little amount cations are doped into polymer chains, an obvious change for the conductivity is observed in Table II. Comparing to the polyaniline doped with H^+ , the conductivity of 1–4 orders of magnitude is observed in these samples doped with Eu^{3+} , Tb^{3+} , and Y^{3+} ions, with values of $3.33S\cdot cm^{-1}$, $1.50 \times 10^{-1} S\cdot cm^{-1}$ and $2.26 \times 10^{-1} S\cdot cm^{-1}$. A similar obviously enhanced conductivity after doping Ag/Ag^+ into aniline and other aromatic amine polymers has also been discovered.^{24,30,31} The conductivity is higher for the polyaniline doped with Eu^{3+} ions than those of PANI doped with Y^{3+} and Tb^{3+} ions. The differences in conductivity may be due to the formation of a good conductive network in the doping polymers. A cross-linking structure is possibly formed by the rare earth ions interaction with adjacent polyaniline chains. In fact, the result of XRD has confirmed that the cooperation of the rare earth ions and the crystalline domains is higher for Y-PANI, Tb-PANI, and Eu-PANI than that of EB, indicating that the PANI tends to organize the polymer chains in highly ordered arrays when rare earth ions interaction with polymer, and the better delocalization of electrons will be produced in the matrix of polyaniline under the influence of the rare-earth cations, so the doped PANI exhibits the increasing conductivity. Additionally, the complex of nitrogen atom with the rare earth ion results in an invalid cluster due to the highly ordered array, it will be in favor of the fluorescence increase. In addition, the conductivity of the doped polymers is affected by their oxidation degree. In the comparing Fe-PANI with Al-PANI case, the samples of Fe-PANI and Al-PANI at the doping ratio for 2.5 display lower conductivity. Their conductivities are 5.74×10^{-2} and $1.61 \times 10^{-1} S\cdot cm^{-1}$, respectively. The lower conductivity is because the Fe^{3+} ions have stronger oxidation than Al^{3+} ions to lead to the higher oxidation degree.

The fluorescence behavior of EB and the doped PANI in NMP is shown in Figure 5. To confirm the effect of the rare earth ions on PANI chains, it is useful to compare the fluorescence of EB with the doped PANI, and two kinds of the rare earth ions with fluorescent characteristic (Eu^{3+} , Tb^{3+}) and non-fluorescent characteristic (Y^{3+}) are chosen. Figure 5(A) presents the excitation spectra of EB and the doped PANI. All samples doped with different cations exhibit three peaks at 275, 310, and 370 nm, regardless of the excitation wavelength. The H-PANI has a very weak peak intensity, however, the peak intensity of excitation of polymer is obviously increased after doping with the rare earth ions, and a small shoulder peak in the doped PANI spectrum

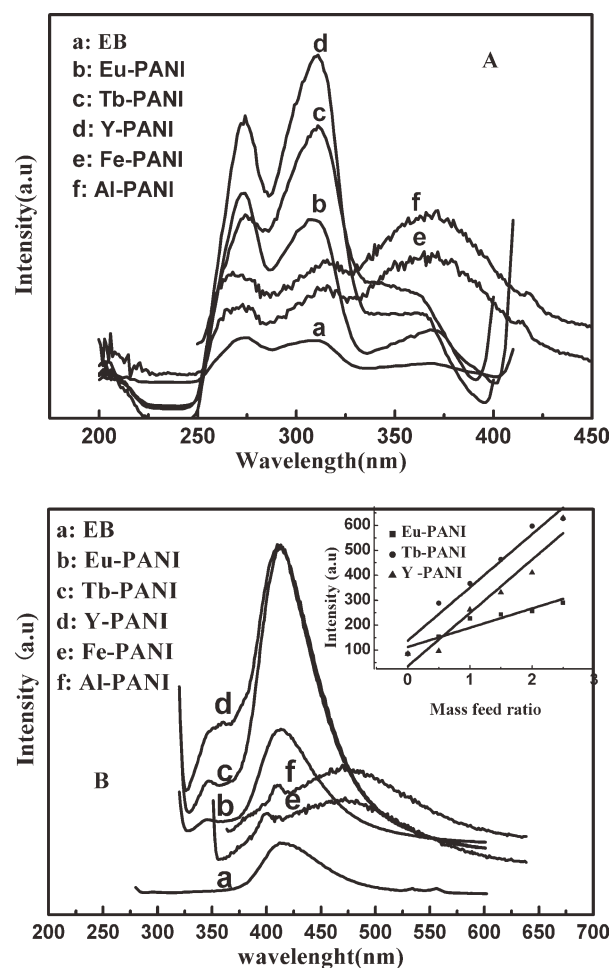


Figure 5 Excitation (A) and Emission (B) spectra of PANI doped with different rare earth ions in NMP. (a) ytterbium ion; (b) terbium ion; (c) europium ion; (d) emeraldine base; (e) aluminum ion; (f) iron ion. The inset of B shows the change of the fluorescent intensity as the mass feed ratio of the rare earth ions to PANI. (■)Eu-PANI; (●)Tb-PANI; (▲)Y-PANI.

located around 370 nm can be attributed to conformational and structural changes of polymeric chains due to the complex of the rare earth ions with nitrogen atoms of imine groups on PANI backbone. The Fe-PANI and Al-PANI have a maximum excitation peak around 370 nm relative to the peak intensity of 275 nm and 310 nm, indicating that more coordination structure is formed in the polymeric chains of polyaniline doped with Fe^{3+} and Al^{3+} ion. Unlike Fe-PANI and Al-PANI, the polyaniline doped with H^+ ion and rare earth ions have maximum excitation peak at 310 nm, reflecting the protonation or pseudo-protonation process is dominated. Under 310-nm excitation, all emission spectra for EB and the PANI doped with the rare earth ions and H^+ ion are shown in Figure 5(B). A strong emission peak at 410 nm was observed in Figure 5(B), which can be attributed to the overlap of benzyl units and the typical of the rare earth ions emission. However, the

fluorescent emission of the rare earth ions solutions depends on polarization of the ion in the field of a ligand or solvate envelop, and it is normally suppressed in a symmetric environment.³² Gradually, the characteristic peaks of the rare earth ions solutions are observed around 500–600 nm, but the interaction of polyaniline with the rare earth ions improved the fluorescent characteristic, indicating that the polymer causes disappearance of characteristic emission peaks of the rare earth ions in the red region and appearance of a broad band centered at 410 nm. An enhanced band for the doped PANI is found by comparing with EB, the result shows that a coordination effect occurs between PANI and the rare earth ions. A new shoulder peak at 350 nm is possibly attributed to the change of the conjugated structure owing to the interaction of the nitrogen atom on PANI chains with the rare earth ions. Moreover, the PANI doped with Y^{3+} ions, which has the same electronic structure with inactive gas, also demonstrated the coordination effect because it is the same as Eu^{3+} and Tb^{3+} ions with only characteristic emission peak after doping Y^{3+} ions. The increasing of fluorescent intensity of polyaniline may originate from a steady plane rigid structure for PANI chains formed by the complexation of nitrogen atoms in polymer chains with Y^{3+} ions. The inset of Figure 5(B) is the function of fluorescent intensity as the mass feed ratio of the rare earth ion to PANI at the range from 0 to 2.5. The addition of the rare earth ions leads to an increase of the fluorescent intensity of the polymer system which is different for each rare earth ion. In each case, a good linear relationship is observed with reversely high correlation coefficient of 0.9525, 0.9804, and 0.9716, corresponding to Eu-PANI, Tb-PANI, and Y-PANI, respectively. The result indicates that rare earth ions can sensitize the fluorescence of PANI through improving the structure of polymeric chains, whereas the fluorescent emission of the rare earth ions disappears in polyaniline environment. The emission peaks of polyaniline doped with Fe^{3+} and Al^{3+} ions at the excitation wavelength of 370 nm are located at 477 nm. Comparing with the protonation process of the H-PANI, a weak emission peak around 410 nm is found in the Fe-PANI and Al-PANI, but their main emission peak shifts to longer wavelength and fluorescent intensity increases due to a steady plane rigid structure formed by complexing Fe^{3+} and Al^{3+} ion with the nitrogen atoms in the polymeric chains. The result indicates that the excitation peaks of polyaniline with Fe^{3+} or Al^{3+} are dominated by the wavelength around 370 nm due to the doping process of polyaniline with Fe^{3+} or Al^{3+} ions that is ascribed to complexation process.

To further confirm the cooperation effect of PANI with the rare earth ion, the rare earth ion at a higher

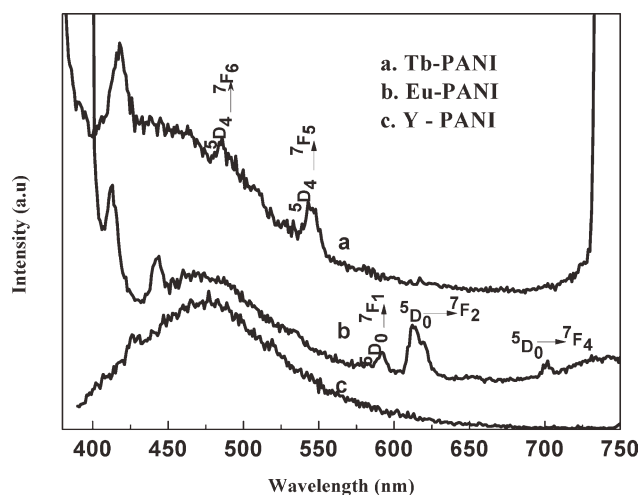


Figure 6 Emission spectra of PANI doped with different rare earth ions at the mass feed ratio of 1 : 40 in NMP. (a) Eu-PANI; (b) Tb-PANI; (c) Y-PANI.

concentration will be investigated in system. The emission spectra of polyaniline doped with the rare earth ions at the ratio of 40 : 1 are shown in the Figure 6. The emission spectrum of Eu-PANI exhibits three emission bands at 593, 613, and 701 nm, assigned to ${}^5D_0 \rightarrow {}^7F_1$, ${}^5D_0 \rightarrow {}^7F_2$ and ${}^5D_0 \rightarrow {}^7F_4$ transitions of Eu(III) ions, respectively. Two emission bands at 486 and 545 nm, assigned to ${}^5D_4 \rightarrow {}^7F_6$ and ${}^5D_4 \rightarrow {}^7F_5$ transitions of Tb(III) ions, are found in the emission spectra of Tb-PANI. Interestingly, the emission peak for Y-PANI shifts to 477 nm at higher concentration, and presents the same emission wavelength with the Fe-PANI and Al-PANI. This indicates the nitrogen atoms in the polymeric chains complex with many more rare earth ions to form a steady plane rigid structure at the higher doping ratio. The results of PANI doped with Eu^{3+} and Tb^{3+} can be attributed to other complex structures leading to energy transfer from the ligand of polyaniline to rare earth ions by Antenna effect. Therefore, the emission intensity of ligand weakens, whereas the characteristic emission intensity of Eu^{3+} and Tb^{3+} ions increases accordingly. However, the most shifted wavelength of PANI doped with Y^{3+} should be ascribed to the close shell f-orbitals of Y^{3+} which do not introduce low-energy metal-centered or charge-separated excited states. Thus one shifted fluorescent emission peak of Y-PANI is found at 477 nm.

CONCLUSION

The doping polyanilines have been prepared in acetonitrile solution containing rare earth cations. Structural analysis indicated that the interactions of PANI with rare earth cations occur at the nitrogen atom of imine groups on polymeric chain backbones. These results led to the increase of delocalization of

conjugated electrons and ordered arrays of polymer chains. The doping content of rare earth cations depends on the mass ratio of PANI to cations and the kinds of rare earth cations. The doping content increases with increasing the concentration of cations at a fixed mass of PANI, and no change was discovered at the mass ratio of cations to PANI for 2.5. The maximum doping content of Eu^{3+} ions is 13.21 wt %. An enhancement of conductivity is demonstrated by improving the doping content of polymer, the conductivity of 1 ~ 4 orders of magnitude is observed in all doping samples contrasting to the protonated polyaniline. Two rare earth cations can significantly increase the fluorescent intensity of polyaniline due to a steady plane rigid structure for PANI chains formed by the complex of nitrogen atoms on polymer chains with Y^{3+} ions. The result indicates that rare earth ions can sensitize the fluorescence of PANI by improving the structure of polymeric chains, whereas the fluorescent emission of rare earth ions disappears in polyaniline environment. However, as the concentration of the rare earth ions increases till 40, the coordination effect becomes the most obvious due to Antenna effect, and the characteristic peak of the rare earth ions can be found. What's more, the emission wavelength of polyaniline will shift to 477 nm, and the peak position is the same as that of Fe-PANI and Al-PANI.

References

1. Sun, L. J.; Liu, X. X. *Eur Polym J* 2008, 44, 219.
2. Ismail, Y. A.; Chang, J.; Shin, S. R.; Mane, R. S.; Han, S. H.; Kim, S. J. *J Electrochem Soc* 2009, 156, A313.
3. Yang, C.; Chen, C. *Synth Met* 2005, 153, 133.
4. Izumi, C. M. S.; Constantino, V. R. L.; Ferreira, A. M. C.; Temperini, M. L. A. *Synth Met* 2006, 156, 654.
5. Sarno, D. M.; Martin, J. J.; Hira, S. M.; Timpson, C. J.; Gaffney, J. P.; Jones, W. E. *Langmuir* 2007, 23, 879.
6. Rivas, B. L.; Sanchez, C. O. *J Appl Polym Sci* 2001, 82, 330.
7. Aguirre, M. J.; Retamal, B. A.; Zanartu, M. S. V.; Zagal, J. H.; Córdova, R.; Schrebler, R.; Biaggio, S. R. *J Electroanal Chem* 1992, 328, 349.
8. Chen, S. A.; Lin, L. C. *Macromolecules* 1995, 28, 1239.
9. Izumi, C. M. S.; Brito, H. F.; Ferreira, A. M. D. C.; Constantino, V. R. L.; Temperini, M. L. A. *Synth Met* 2009, 159, 377.
10. Ryu, K. S.; Moon, B. W.; Joo, J. S.; Chang, S. H. *Polymer* 2001, 42, 9355.
11. Dimitriev, O. P.; Kislyuk, V. V. *Synth Met* 2002, 132, 87.
12. Izumi, C. M. S.; Ferreira, D. C.; Ferreira, A. M. D. C.; Temperini, M. L. A. *Synth Met* 2009, 159, 1165.
13. Chen, Z. X.; Shen, Z. Q. *Inorg Chem Acta* 1986, 122, 249.
14. Shipley, C. P.; Capecchi, S.; Salata, O. V.; Etchells, M.; Dobson, P. J.; Christou, V. *Adv Mater* 1999, 11, 533.
15. Sun, T.; Bi, H.; Zhu, K. R. *Spectrochim Acta A* 2007, 66, 1364.
16. Kim, Y. H.; Foster, C.; Chiang, J.; Heeger, A. J.; *Synth Met* 1989, 285, 27.
17. Chiang, J. C.; MacDiarmid, A. G. *Synth Met* 1986, 13, 193.
18. Drelkiewicz, A.; Hasik, M.; Choczynski, M. *Mater Res Bull* 1998, 33, 739.
19. Louarn, G.; Lapskowski, M.; Quillard, S.; Pron, A.; Buisson, J. P.; Lefrant, S. *J Phys Chem* 1996, 100, 6998.
20. Yang, C. M.; Zhang, Q. R.; Fang, Z. *Acta Metallurgica Sinica* 2000, 13, 872.
21. Li, X. G.; Lu, Q. F.; Huang, M. R. *Small* 2008, 4, 1201.
22. Li, X. G.; Li, A.; Huang, M. R. *Chem Eur J* 2008, 14, 10309.
23. Li, X. G.; Feng, H.; Huang, M. R. *Chem Eur J* 2009, 15, 4573.
24. Li, X. G.; Feng, H.; Huang, M. R. *Chem Eur J* 2010, 16, 10113.
25. Ng, S. W.; Neoh, K. G.; Sampanthar, J. T.; Kang, Y. T.; Wong, K. L. Tan, J. *Phys Chem B* 2001, 105, 5618.
26. Gunnlaugsson, T.; Lee, T. C.; Parkesh, R. *Tetrahedron Lett* 2004, 60, 11239.
27. Albuquerque, J. E.; Mattoso, L. H. C.; Balogh, D. T.; Faria, R. M.; Masters, J. G.; MacDiarmid, A. G. *Synth Met* 2000, 113, 19.
28. Yang, Y. S.; Wan, M. X. *J Mater Chem* 2002, 12, 897.
29. Pouget, J. P.; Jdzefowicz, M. E.; Epstein, A. J.; Tang, X.; MacDiarmid, A. G. *Macromolecules* 1991, 24, 779.
30. Li, X. G.; Liu, R.; Huang, M. R. *Chem Mater* 2005, 17, 5411.
31. Li, X. G.; Ma, X. L.; Sun, J.; Huang, M. R. *Langmuir* 2009, 25, 1675.
32. Gallagher, P. K. *J Chem Phys* 1964, 41, 3061.